

NUMERICAL SIMULATION OF IMPACT ON A CRACKED PLATE

NUMERIČKA SIMULACIJA UDARA O PLOČU SA PRSLINOM

Originalni naučni rad / Original scientific paper

Rad primljen / Paper received: 3.12.2024

<https://doi.org/10.69644/ivk-2026-01-0070>

Adresa autora / Author's address:

¹⁾ Mechanical Engineering Department, University of Relizane, 48000, Algeria, S. Kerrouz <https://orcid.org/0000-0001-9957-0203>, *email: Kerrouzsiham@gmail.com

²⁾ Mechanical Physical Materials Laboratory (LMPM), Mechanical Engineering Department, University of Sidi Bel-Abbes 22000, Algeria L. Zouambi <https://orcid.org/0000-0002-1732-5237>

³⁾ Mechanical Engineering Department, University Center of Maghnia, Tlemcen, Algeria M. Bourdim <https://orcid.org/0009-0007-2958-9700>

Keywords

- cracked plate
- impact
- dynamic
- ANSYS LS Dyn
- spherical projectile

Abstract

To predict the dynamic behaviour of structures under the effect of impact, we approach the dynamic problem in the form of a numerical simulation of impact on a cracked plate. Our choice is focused on a numerical simulation in order to examine the response of a cracked aluminium alloy plate impacted by a spherical steel projectile. The use of ANSYS[®] LS Dyn (dynamic explicit) software allows us to study this behaviour as a function of the boundary conditions, and the geometric parameters of a plate and the sphere, taking into account the variation of the crack length. A comparison is made with the case of a healthy plate without defects dynamically stressed under the same conditions. In addition, the calculation of the equivalent Von Mises stresses and equivalent elastic deformations are carried out.

INTRODUCTION

The fathers of linear fracture mechanics are recognised as Griffith (1893-1963) and Irwin (1907-1998). The first perception by man of the phenomenon of fracture dates back to the prehistoric era and the manufacture of tools by flint cutting (brittle fracture by cleavage). Until the 16th century, the phenomenon of fracture was used mainly for the extraction of blocks of material for construction (Egyptian pyramids and obelisks, Mesoamerican temples and pyramids, cathedrals and Middle Ages constructions, etc.) or the manufacture of tools (Gallo-Roman millstones).

Several analytical and experimental studies have investigated the elastic impact of perfectly fitted laminates. Moriarty and Goldsmith /1/ conducted experimental investigation on the dynamic energy absorption characteristics of structures. Minak and Ghelli /2/ studied the influence of diameter and boundary conditions on the low velocity impact response of circular CFRP laminated plates. The tests indicated that the dimensions and boundary conditions influence the impact behaviour of the material, as they affect the stiffness of the target. Craven, Sztefek, and Olsson /3/ conducted research on impact damage in multidirectional structures and its effects on local tensile stiffness. The important

Ključne reči

- ploča sa prslinom
- udar
- dinamičko ponašanje
- ANSYS LS Dyn
- sferni projektil

Izvod

Radi predviđanja dinamičkog ponašanja konstrukcija pod dejstvom udara, mi pristupamo dinamičkom problemu putem numeričke simulacije udara o ploču sa prslinom. Naš izbor se fokusira na numeričku simulaciju kako bi se proučio odziv ploče sa prslinom od legure aluminijuma, posle sudara sa sfernim čeličnim projektilom. Primena softvera ANSYS[®] LS Dyn (dynamic explicit) omogućava nam da istražimo ovo ponašanje u funkciji graničnih uslova, kao i geometrijskih parametara ploče i sfere, uzimajući u obzir varijacije dužine prsline. Izvedeno je poređenje ovog slučaja sa pločom bez grešaka, koja je takođe podvrgnuta dinamičkom opterećenju u istim uslovima. Pored toga, izveden je proračun ekvivalentnih Von Misesovih napona i ekvivalentnih elastičnih deformacija.

parameters of impact damage under tensile loading were identified as crack failures.

However, risks associated with the dynamic propagation of cracks under impact are still very difficult to estimate. On the one hand, although many experiments have already been carried out, obtaining experimental results remains tricky, particularly if we are looking for specific loading and propagation conditions. On the other hand, numerical simulation tools for dynamic crack propagation are still few in number, and it is difficult to use and integrate rudimentary propagation criteria, /4/.

If materials contain a number of microcracks that become unstable and lead to fracture when the applied stress exceeds a critical value. To understand this behaviour, it is necessary to analyse in detail the phenomena occurring at the tip of a crack. The study of the behaviour of a crack under stress forms the basis of fracture mechanics, /5, 6/.

LINEAR ELASTIC FRACTURE MECHANICS (LEFM)

The determination of σ and ε , in a cracked structure uses classical methods in mechanics, but they are difficult to use. Two particular stress states can be distinguished: the plane stress state and the plane strain state. We find ourselves in a plane stress state, for example, in a thin sheet subjected to

forces in its plane. The plane strain state can take place at the centre of a thick part, where the triaxiality of the stresses is significant.

Plane stresses

We say that we are in a state of plane constraints if all the components along the direction of the Z axis (for example) are zero /5/:

$$\sigma_{ZZ} = \tau_{XZ} = \tau_{YZ} = 0. \tag{1}$$

The other components of stresses and strains along the X, Y axes are given by Hooke's law as follows:

$$\begin{bmatrix} \sigma_{XX} \\ \sigma_{YY} \\ \tau_{XY} \end{bmatrix} = \frac{E}{(1-\nu^2)} \begin{bmatrix} 1 & \nu & 0 \\ \nu & 1 & 0 \\ 0 & 0 & \frac{1-\nu}{2} \end{bmatrix} \begin{bmatrix} \varepsilon_{XX} \\ \varepsilon_{YY} \\ 2\varepsilon_{XY} \end{bmatrix}, \tag{2}$$

or else:

$$\{\sigma\} = [D]\{\varepsilon\}, \tag{3}$$

$$\varepsilon_{XX} = \frac{1}{E}(\sigma_{XX} - \nu\sigma_{YY}), \tag{4}$$

$$\varepsilon_{YY} = \frac{1}{E}(\sigma_{YY} - \nu\sigma_{XX}), \tag{5}$$

$$\varepsilon_{ZZ} = -\frac{\nu}{E}(\sigma_{XX} + \sigma_{YY}), \tag{6}$$

$$\gamma_{XY} = \frac{\tau_{XY}}{2\mu} = \frac{(1+\nu)}{E} \tau_{XY}, \tag{7}$$

$$\gamma_{YZ} = \gamma_{ZX} = 0. \tag{8}$$

The plane stress state is encountered in the case of a thin plate, loaded in its plane, from where the dimension along Z is negligible compared to dimensions in the plane (XY) /6/.

Plane deformations

We say that we are in a state of plane deformation if the deformation preserves the flatness of any straight section perpendicular to the Z axis.

The conditions for a plane deformation state are:

- out-of-plane deformations:

$$\varepsilon_{ZZ} = \varepsilon_{XZ} = \varepsilon_{YZ} = 0, \tag{9}$$

- the two transverse shear stresses in the plane are zero:

$$\tau_{XZ} = \tau_{YZ} = 0. \tag{10}$$

The other components of stresses and strains along the X, Y axes are given by Hooke's law according to the following expressions:

$$\begin{bmatrix} \sigma_{XX} \\ \sigma_{YY} \\ \tau_{XY} \end{bmatrix} = \frac{E}{(1+\nu)(1-2\nu)} \begin{bmatrix} 1-\nu & \nu & 0 \\ \nu & 1-\nu & 0 \\ 0 & 0 & \frac{1-2\nu}{2} \end{bmatrix} \begin{bmatrix} \varepsilon_{XX} \\ \varepsilon_{YY} \\ 2\varepsilon_{XY} \end{bmatrix}, \tag{11}$$

or else:

$$\{\sigma\} = [D]\{\varepsilon\}, \tag{12}$$

$$\sigma_{ZZ} = \nu(\sigma_{XX} + \sigma_{YY}), \tag{13}$$

$$\varepsilon_{XX} = \frac{1}{E}[(1-\nu^2)\sigma_{XX} - \nu(1+\nu)\sigma_{YY}], \tag{14}$$

$$\varepsilon_{YY} = \frac{1}{E}[(1-\nu^2)\sigma_{YY} - \nu(1+\nu)\sigma_{XX}], \tag{15}$$

$$\varepsilon_{XY} = \frac{\tau_{XY}}{2\mu} = \frac{(1+\nu)}{E} \tau_{XY}. \tag{16}$$

The plane stress hypothesis implies $\varepsilon_{ZZ} = -\nu(\sigma_{XX} + \sigma_{YY})/E$ that is therefore singular in $r^{-1/2}$, but the compatibility Eqs.

(8) require that it is linear in X and Y and therefore regular. This incompatibility does not exist in the plane strain solution.

The elementary cracking mode I used in this study (Fig. 1) that is, the two surfaces of the crack move relative to each other in a direction perpendicular to the plane of the crack. It is similar to the displacement produced by a rectangular corner dislocation parallel to the crack front whose Burgers vector is parallel to the displacement.

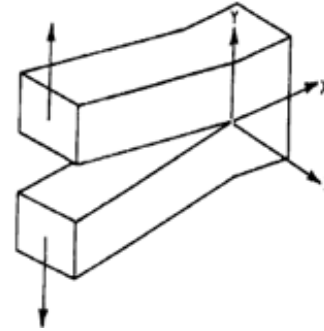


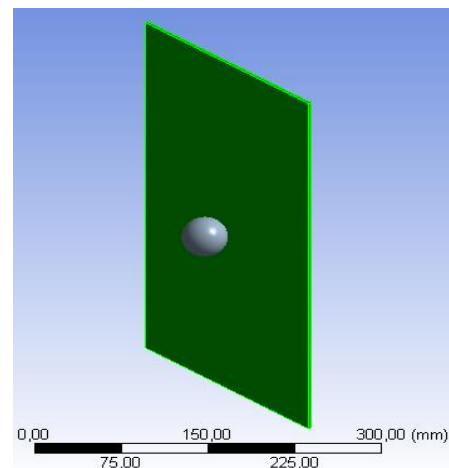
Figure 1. Mode I crack opening.

NUMERICAL SIMULATION

This research is part of the study of the behaviour of a cracked plate subjected to the impact of a spherical projectile using the ANSYS calculation code. The aim is to analyse the impact phenomenon and its effect on plates in general and cracked plates in particular, and to make a comparison between the two types. For the numerical simulation, the two 200x400x3 mm³ flexible aluminium plates are impacted by a rigid spherical steel projectile of mass 0.26306 kg and 40 mm in diameter. The cracked plate contains two cracks at the edges. The behaviour of the two plates during impact is analysed in terms of equivalent elastic stresses and deformations. The influence of crack size on the dynamic response of the plate is also discussed.

For comparison purposes, the two plate types are distinguished: an uncracked plate (Fig. 2), and a plate cracked on both edges (Fig. 3).

The geometric models of the two plates and the spherical projectile are designed with Solidworks® 2016 for analysis and saved in *.igs file format, then imported into ANSYS® Workbench.



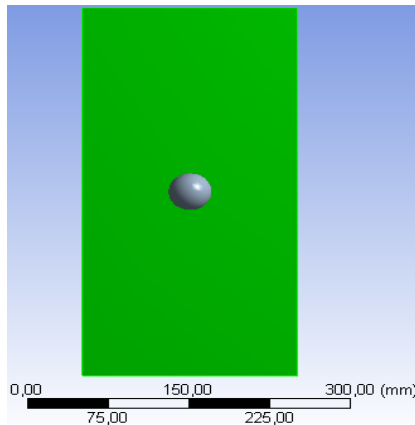


Figure 2. Geometric model of the uncracked plate.

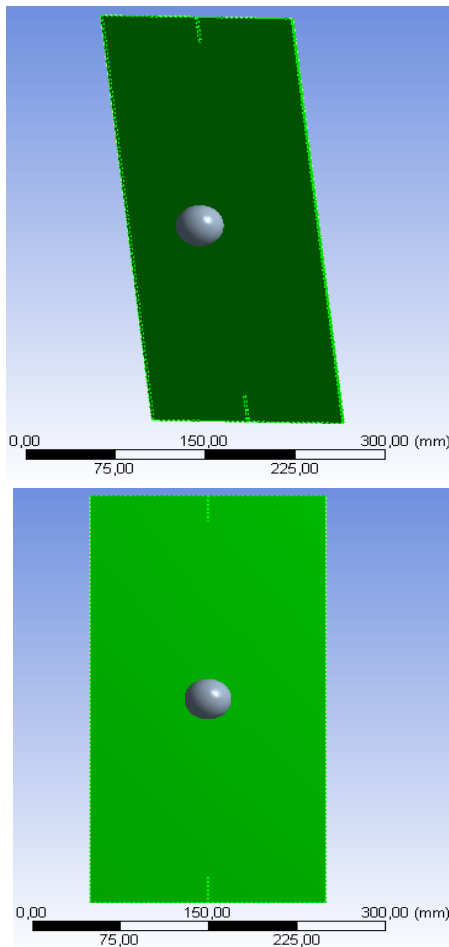


Figure 3. Geometric model of the cracked plate.

Table 1. Sizes of the plate and sphere.

Structures	Sizes
Plates (targets)	length $L = 400$ mm, width $l = 200$ mm, thickness $t = 3$ mm
Spheres (projectiles)	radius $R = 15$ mm
Initial distance between plate and sphere	$d = 10$ mm

Materials of the three geometries

In this study, high carbon FG25 gray cast iron, with good conductivity, fairly good mechanical strength and low wear /7-9/ is chosen for the spherical projectile, and aluminium for both plates. Table 2 summarises their properties.

Table 2. Mechanical properties of spherical steel projectile and aluminium plates, /10/.

Material	Density ρ (kg/m ³)	Young's modulus E (N/m ²)	Poisson's ratio ν	Mass m (kg)
Al alloy plate	2770	$7 \cdot 10^{10}$	0.33	0.66463
steel projectile	7850	2^{11}	0.3	0.263

Creating a mesh using finite elements

A mesh can be defined as a discretisation of geometry into small subdomains. A mesh can be triangular with 4 nodes. The subdomains are often called elements or cells, and the collection of all elements or cells is called a mesh or grid, and physics calculates the appropriate parameters for each node point, /11/.

Figure 4 shows the volume mesh of both the cracked and uncracked plate, respectively. This mesh uses 2130 nodes and 3805 elements for the cracked plate, and 2132 nodes and 3814 elements for the uncracked plate. The models are analysed and crushed to obtain the results of equivalent stresses and equivalent elastic strains.

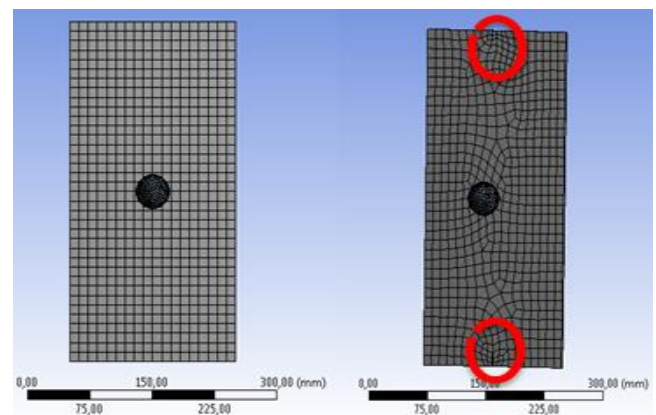
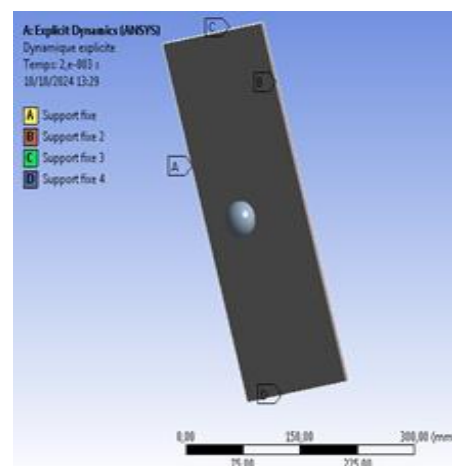


Figure 4. Uncracked- and cracked plate mesh.

Assuming that:

- plates are flexible while the sphere is a rigid body;
- cracked plate is embedded on the two uncracked edges;
- distance between the sphere and the plate is 10 mm;
- impact speed is 2.5 m/s;
- impact duration is $t = 0.002$ s;
- crack length is $a/w = 0.075$,

the loading and boundary conditions are defined as shown in Figs. 5 and 6, whereas impact speed is shown in Fig. 7.



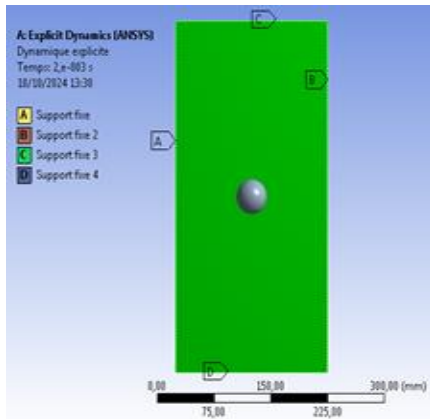


Figure 5. Loading and boundary conditions of uncracked plate.

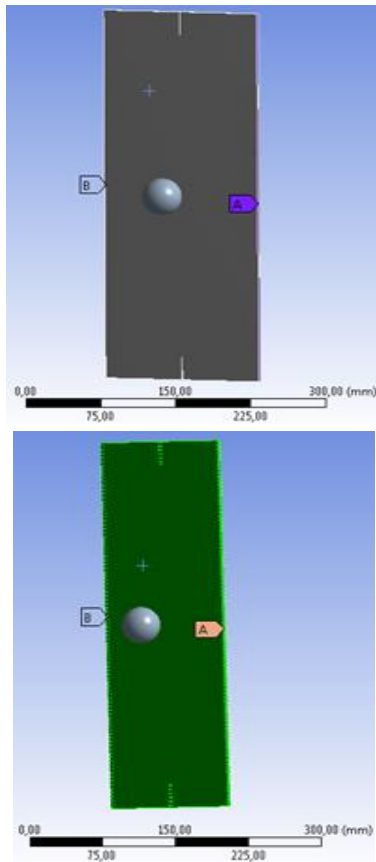


Figure 6. Loading and boundary conditions of cracked plate.

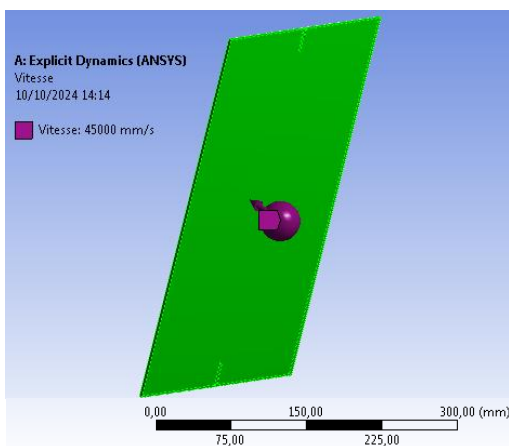


Figure 7. Impact speed.

RESULTS AND DISCUSSION

Comparison of the distribution of the equivalent Von Mises stress field between the two impacted plates

During impact and when the plate is in contact with the spherical projectile, the comparison between the results of these two types shows that a high concentration of stresses is located at the contact zone of the uncracked plate with a maximal value of 98.3 MPa that gradually decrease to the corners of the plate edges but with a minimal value of 7.4 MPa, Fig. 8.

In the case of the cracked plate impacted by the sphere, results show that the maximal equivalent stress, 344.2 MPa, is located near the crack tip and then it gradually decreases towards the free edges of the crack, Fig. 9. In addition, the stresses in the vicinity of the contact point are very low.

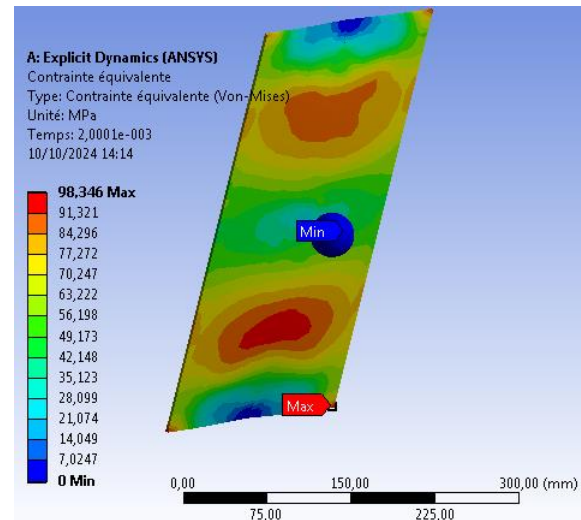


Figure 8. Distribution of Von Mises stresses in the uncracked plate.

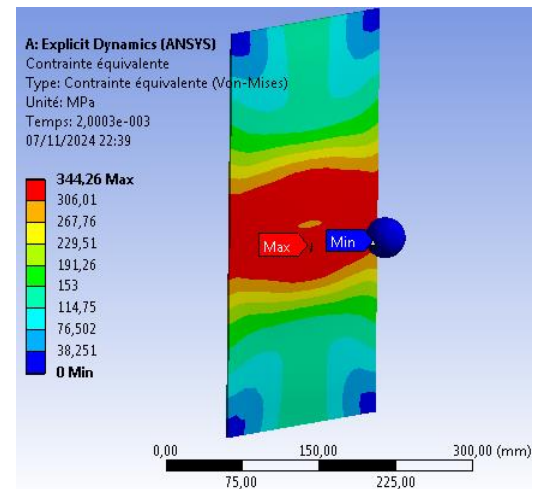


Figure 9. Distribution of Von Mises stresses in the cracked plate.

Influence of crack length variation on equivalent stress field variation

Under the effect of changing the crack length, respectively $a/w = 0.063$; 0.075 ; 0.1 and under the same boundary conditions as used previously, Fig. 10 shows that in each of these 3 variants one can see that the equivalent stresses are concentrated mainly near the crack tip and then gradually decrease towards the free edges of the crack.

The maximal value of equivalent stress appears in the cracked plate with a length of $a/w = 0.1$.

It can be concluded that the variation of crack length has an influence on the equivalent stress distribution during the impact.

Curves of equivalent Von Mises stresses have the same appearance, Fig. 11, as they go through three phases: the first phase includes two stages - the first stage corresponds to the contact between the plate and sphere; and in the second stage the level of stresses rises with damage caused from the dif

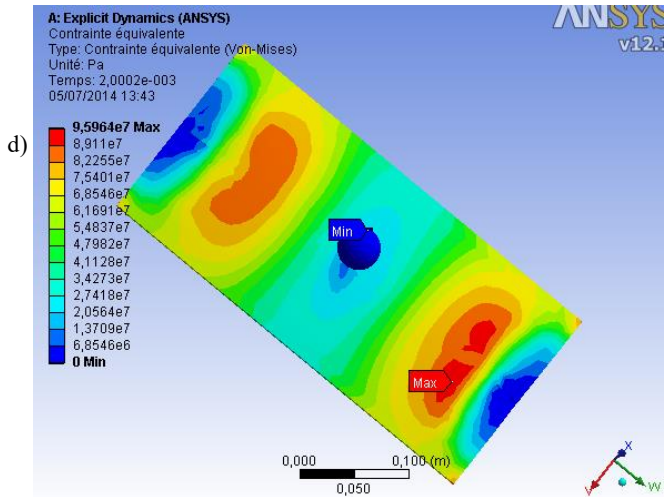
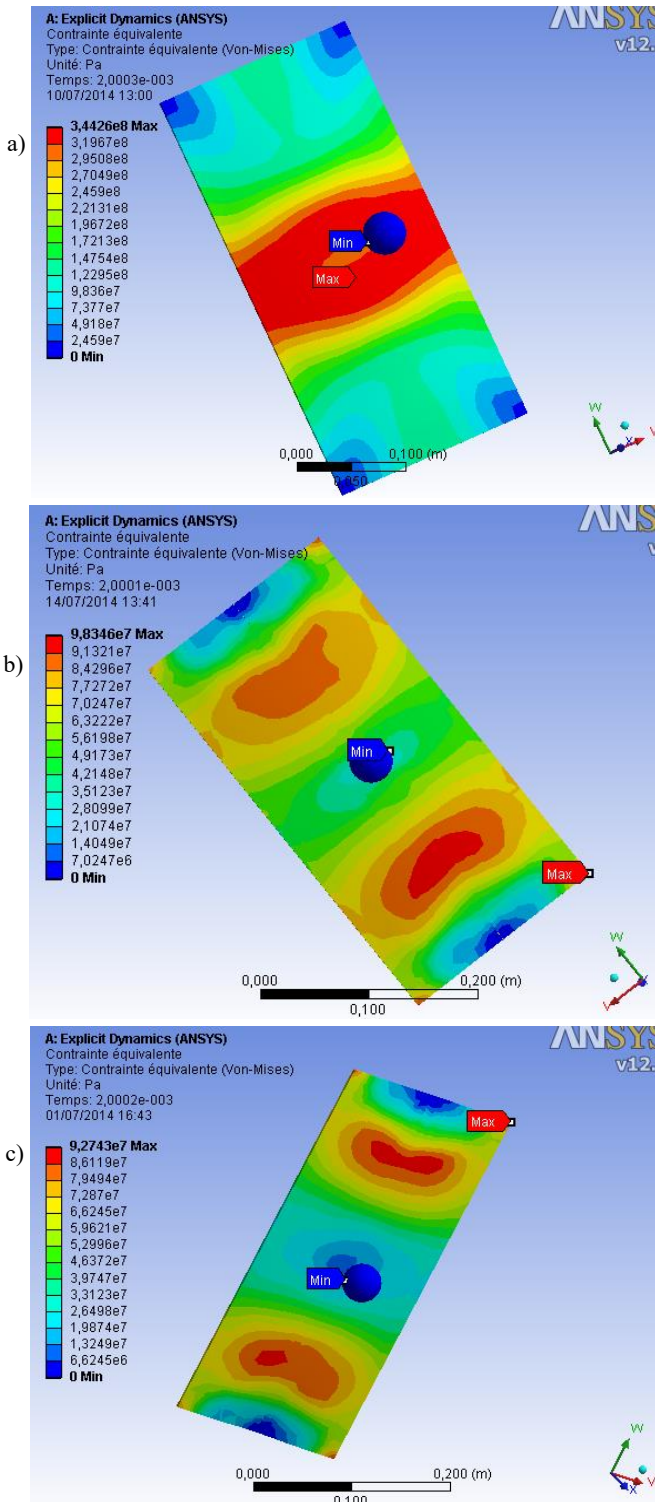


Figure 10. Influence of crack length variation on the variation of Von Mises equivalent stress distribution: a) $a/w = 0$; b) $a/w = 0.063$; c) $a/w = 0.075$; d) $a/w = 0.1$.

ference between potential and kinetic energy of the two structures (the energy of the impactor being greater than that of the plate). In the second phase the damage is present with stress peaks. In the third phase the damage threshold or part of the energy is used to make the impactor rise, this is the rebound phenomenon.

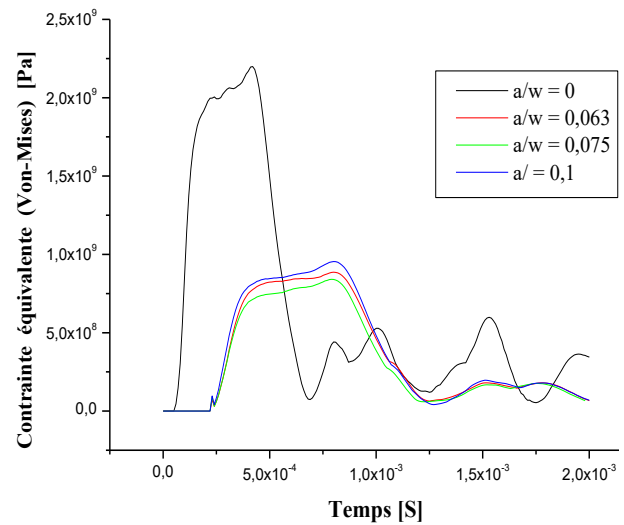


Figure 11. Von Mises stresses with an impact velocity of 2.5 m/s as a function of the variation of crack length.

Influence of impact velocity variation on the variation of Von Mises equivalent stress

Under the effect of change of impact velocity, respectively $v = 1, 1.5, 2, 2.5,$ and 3 m/s under the same boundary conditions used previously. Figure 12 shows that for each of 5 variants, it is observed that the equivalent stress increases with the increase of impact velocity. It can also be noticed that the equivalent stress decreases rapidly after initial impact. It can be concluded that the variation of impact velocity influences the distribution of equivalent stress during impact.

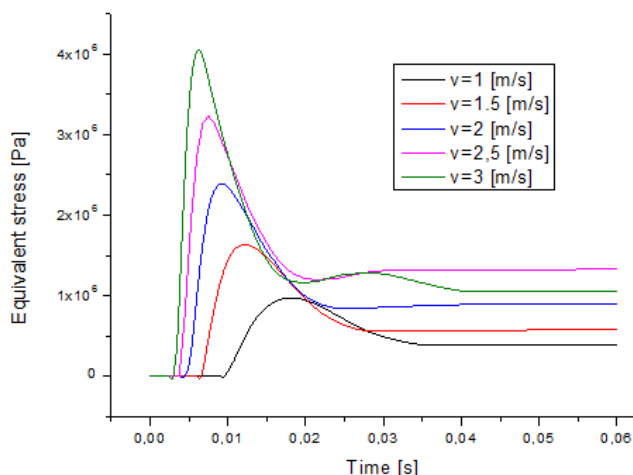


Figure 12. Variation of equivalent stress as a function of variation in impact speed.

CONCLUSIONS

This work is part of the dynamic impact analysis on a cracked plate. The study made it possible to understand the behaviour of a healthy plate and a cracked plate under the effect of a dynamic impact of the spherical projectile type. A calculation of dynamic stress intensity factors for the case of different crack lengths is carried out. Modelling, discretisation and dynamic calculation are performed using the finite element calculation code ANSYS Workbench. It is found that the healthy plate has a higher dynamic behaviour than that of an identical plate cracked at the edges.

For the uncracked plate, at the moment of impact, the stresses are maximal around the point of contact while for the cracked plate; these are maximal in the vicinity of the crack tips.

The increase in edge crack length has an influence on the dynamic behaviour of the cracked plate through the evolution of equivalent stresses.

The variation of the impact speed has an influence on the distribution of the equivalent stress during the impact.

REFERENCES

- Moriarty, K., Goldsmith, W. (1993), *Dynamic energy absorption characteristics of sandwich shells*, Int. J Impact Eng. 13(2): 293-317. doi: 10.1016/0734-743X(93)90098-R
- Minak, G., Ghelli, D. (2008), *Influence of diameter and boundary conditions on low velocity impact response of CFRP circular laminated plates*, Compos. Part B: Eng. 39(6): 962-972. doi: 10.1016/j.compositesb.2008.01.001
- Craven, R., Sztefek., P., Olsson, R. (2008), *Investigation of impact damage in multi-directional tape laminates and its effect on local tensile stiffness*, Compos. Sci. Technol. 68(12): 2518-2525. doi: 10.1016/j.compscitech.2008.05.008
- Muskhelishvili, N.I., *Some Basic Problems of the Mathematical Theory of Elasticity* (translated from Russian by J.R.M. Radok), Oxford University Press, Bombay, 1953.
- Pluinage, G., *Mécanique élastoplastique de la rupture, critères d'amorçage*, Cépadués-éd., Paris, 1989. ISBN 978-2-85428-220-7
- Rokbi, M., *Comportement a la rupture et caractérisation mécanique de composites polyester-fibres de verre*, Mémoire de magister, Centre Universitaire Mohamed Boudiaf de M'Sila, Institut de Génie Mécanique, Algerie, 2001.

- Oder, G., Reibenschuh, M., Lerher, T., et al. (2009), *Thermal and stress analysis of brake discs in railway vehicles*, Int. J Adv. Eng. 3(1): 95-102.
- Jang, H., Ko, K., Kim, S.J., et al. (2004), *The effect of metal fibers on the friction performance of automotive brake friction materials*, Wear, 256(3-4): 406-414. doi: 10.1016/S0043-1648(03)00445-9
- Kerrouz, S., Bourdim, M., Tamine, T., Bouchetara, M. (2021), *Study of the mechanical behavior of an automobile brake disc*, Period. Polytech. Mech. Eng. 65(3): 197-204. doi: 10.3311/PPme.15589
- Kerrouz, S., *Etude dynamique d'impact sur une plaque fissure*, mémoire de magister, Université des Sciences et de la Technologie d'Oran Mohamed Boudiaf, Algerie, 2014.
- Kerrouz, S., *Comportement thermo-élastique des contacts glissants secs - Approche numérique*, thèse de doctorat, Université des Sciences et de la Technologie d'Oran Mohamed Boudiaf, 2024.

© 2026 The Author. Structural Integrity and Life, Published by DIVK (The Society for Structural Integrity and Life 'Prof. Dr Stojan Sedmak') (<http://divk.inovacionicentar.rs/divk/home.html>). This is an open access article distributed under the terms and conditions of the [Creative Commons Attribution-NonCommercial-NoDerivatives 4.0 International License](https://creativecommons.org/licenses/by-nc-nd/4.0/)